

Enantioselective Adsorption in Achiral Zeolites**

Titus S. van Erp,* Tom P. Caremans, David Dubbeldam, Ana Martin-Calvo, Sofia Calero, and Johan A. Martens

The separation of mixtures of chiral compounds into their left- and right-handed forms is of vital importance for the pharmaceutical and agrochemical industries.^[1] For decades, extensive research has been devoted to the development of chiral separation processes. Zeolites contain channels and cages of molecular dimensions and therefore are ideally suited for molecular separation.^[2] However, chiral zeolites are scarce.^[3–5] Here, we demonstrate, by means of computer simulations, the enantioselective adsorption of 4-ethyl-4-methyloctane in aluminosilicate MFI zeolites containing positively charged ions. Our results are remarkable, as the fixed crystallographic zeolite framework is perfectly mirror symmetric. This overthrows the general belief that enantioselective adsorption requires a chiral adsorbent. The nonlocal enantioselective correlations characteristic of this system are induced by packing into hydrocarbon–cation pairs at the channel intersections and by long-range repulsions between cations. Our findings have important technological consequences, as they open perspectives for a whole new approach to enantioseparation.

4-Ethyl-4-methyloctane is the simplest chiral saturated hydrocarbon with a quaternary stereogenic center. It consists of a central carbon with methyl, ethyl, propyl, and butyl groups tetrahedrally attached such that either the *S* or the *R* enantiomer is formed. Zeolite MFI, which has a network of straight and zigzag channels, preferentially adsorbs branched hydrocarbons at the intersections, where their branches can each be located in a separate exit channel. Zeolite MFI has 12

crystallographically different silicon positions, which form the smallest building block, the asymmetric unit, from which one can create the complete unit cell and hence the whole crystal. We focus on homogeneous distributions in which one of these silicon positions is systematically replaced by aluminum to give an Si/Al ratio of 11/1 (8 Al atoms per unit cell). This is close to the maximum concentration of Al atoms achieved in known MFI zeolite materials.^[6] Four of these structures violate the Löwenstein rule, which forbids the presence of Al–O–Al linkages, and were excluded. We name the remaining structures Al-1, Al-2, Al-3, Al-4, Al-5, Al-6, Al-8, and Al-11 after the index^[7] of the substituted site. Replacement of Si⁴⁺ by Al³⁺ results in a negatively charged site in the crystal framework, which is compensated by the inclusion of non-framework Na⁺ or Ca²⁺ cations.

A united-atom force field was used to describe the interactions between the CH_x groups^[8] and mobile cations^[9,10] within a rigid zeolite framework.^[11] The total simulation box consisted of 2 × 2 × 2 unit cells with periodic boundaries. First, we calculated adsorption isotherms at 298 K in the grand-canonical ensemble for an enantiopure gas using the configurational bias Monte Carlo technique (CBMC).^[12] CBMC “grows” the molecules into the zeolite rather than simply inserting them, which would yield a vanishingly low success rate. Above 1 Pa all aluminum silicate systems are in the saturation regime with a constant total number of hydrocarbon molecules of four per unit cell.^[13] Then we switched to mixtures in which the *S* fraction in the external reservoir was set at 0.1, 0.2, ..., or 0.9. Whenever the maximum loading was reached, addition and deletion moves attained zero acceptance and were from there on discarded, effectively converting the system into the semi-grand canonical ensemble; the total number of adsorbed molecules remains constant, but individual numbers of *R* or *S* hydrocarbon molecules can still vary. We performed a series of different Monte Carlo moves comprising translations, rotations, and replacements using CBMC. Only in the last-named can the chirality of the molecule change. In addition, we developed two new Monte Carlo moves^[14] that can change the identity of several molecules in a single step. The last two moves were requisite to obtain highly converged results.

Figure 1 shows the fraction of adsorbed *S* molecules as function of the same enantiomeric ratio in the gas phase for the cases Al-1(Na⁺), Al-2(Na⁺), Al-4(Na⁺), and Al-5(Ca²⁺). The significant deviation of the last three curves from the straight line implies a difference in the fraction of *S* enantiomer that is adsorbed in the zeolite relative to the gas phase. Besides, Al-3(Ca²⁺), Al-5(Na⁺), and Al-6(Ca²⁺) also show absolute differences of more than 5% from the linear curve. No significant deviations were found for Al-1(Ca²⁺),

[*] Dr. T. S. van Erp, Dr. T. P. Caremans, Prof. J. A. Martens
Centrum voor Oppervlaktechemie en Katalyse, K.U. Leuven
Kasteelpark Arenberg 23, 3001 Leuven (Belgium)
E-mail: titus.vanerp@biw.kuleuven.be
Homepage: <http://www.van-erp.org/>

Dr. D. Dubbeldam
Van't Hoff Institute for Molecular Sciences
University of Amsterdam
Nieuwe Achtergracht 166, 1018 WV Amsterdam (The Netherlands)
A. Martin-Calvo, Prof. S. Calero
Department of Physical, Chemical, and Natural Systems
University Pablo de Olavide
Ctra. Utrera km. 1, 41013 Seville (Spain)

[**] We acknowledge the Flemish Government for long-term structural support via the centre of excellence (CECAT), the concerted research action (GOA), and Methusalem funding. T.P.C. acknowledges the Flemish IWT for a PhD grant. T.S.v.E. and J.A.M. participated in interuniversity attraction pole (IAP). S.C. acknowledges the funding via the CTQ2007-63229 and P07-FQM-02595 projects. A.M.C. was supported by a SIMBIOMA grant from the ESF. We thank Paolo Pescarmona for useful remarks.



Supporting information for this article is available on the WWW under <http://dx.doi.org/10.1002/anie.200906083>.

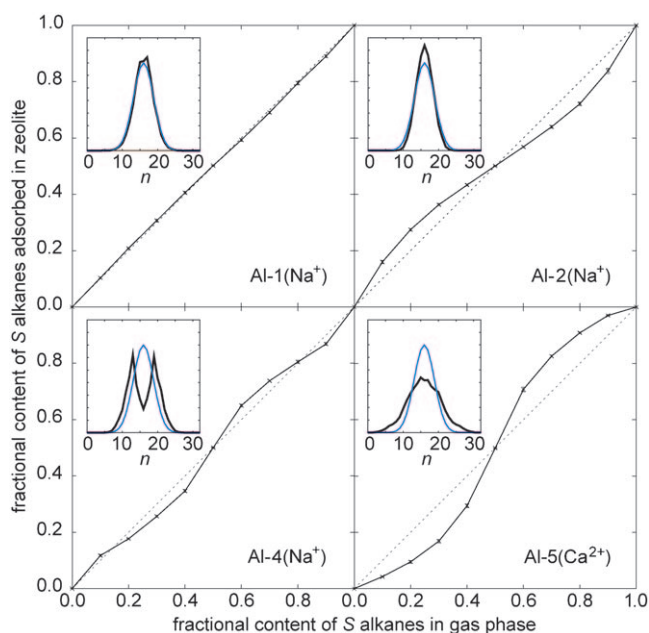


Figure 1. Adsorbed fractional content of the *S* enantiomer versus the same fraction in the external gas phase for four MFI silicates. Insets show the probability distributions $P(n)$ of having exactly n alkane molecules of the left-handed form in the zeolite in case of a racemic (50% *S*, 50% *R*) external gas. The blue curves show the binomial distribution, which is the theoretical result for nonenantiospecific adsorption. All curves are symmetric and pass through (0.5,0.5), which is a direct result of the zeolites' being not chiral by themselves. However, if one enantiomeric form is more available in the reservoir, its relative fraction that is adsorbed may either be higher [Al-5(Ca²⁺)], lower [Al-2(Na⁺)], or either depending on the relative concentration [Al-4(Na⁺)]. Al-1(Na⁺) is not enantioselective.

Al-3(Na⁺), Al-4(Ca²⁺), Al-6(Na⁺), Al-8(Na⁺,Ca²⁺), Al-11(Na⁺,Ca²⁺), and pure-silica MFI. Al-2(Ca²⁺) shows a modest but significant effect (3.5%). Interestingly, inclusion of Ca²⁺ seems to establish an effective homophilic interaction between the alkane molecules, while it is merely heterophilic for Na⁺. In the first situation the adsorbed molecules tend to increase the fraction that is dominant in the reservoir. In the second case, the adsorbate tries to level the enantiomeric ratio towards that of racemic mixture. Al-4(Na⁺) is a special case showing three intermediate intersections with the diagonal and a number distribution that is sharply bimodal. The largest absolute deviation (13%) is found for the Al-5(Ca²⁺) system, on which we will concentrate.

Figure 2 shows two snapshots for the pure-Si MFI zeolite and Al-5(Ca²⁺) for a gas enantiomer ratio of *S*/*R* = 30/70. In all-silica MFI, steric hindrance excludes butyl chains pointing towards each other in the same zigzag channel. Besides, there is no detectable preferred orientation or correlation between neighboring molecules. In contrast, the Al-5(Ca²⁺) system is remarkably ordered. Not only do the *R* alkanes dominate much more than expected considering the molecular content of the reservoir (30 out of 32 molecules are right-handed in this figure), but also all *R* molecules show an almost identical orientation. Butyl and methyl groups are aligned along the zigzag channel with all butyl chains pointing in the same

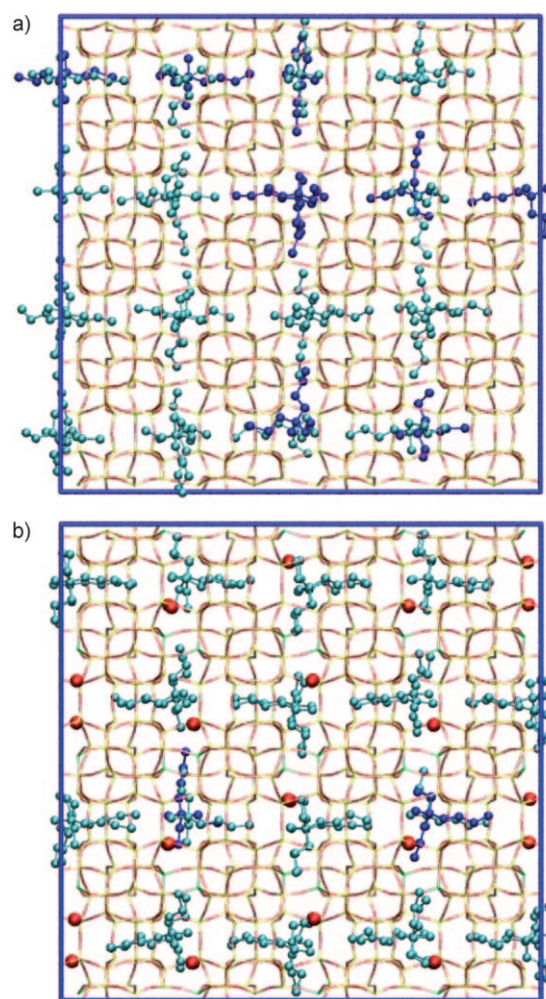


Figure 2. Two configurations of adsorbed 4-ethyl-4-methyloctane (*S*/*R* ratio = 3/7) in a) all-silica MFI and b) Al-5(Ca²⁺). Zigzag and straight channels are respectively horizontal and vertical with respect to the plane of the page. *S* and *R* enantiomers are colored dark and light blue. The red spheres in (b) represent the Ca²⁺ cations.

direction. The ethyl and propyl groups are positioned along the straight channels with the latter always pointing away from the cation. The only molecules not following this pattern are the *S* molecules, which create unavoidable mismatches and their orientation is somewhat unpredictable. Apparently, if the pattern must be broken it does not matter how this is done. Also the cations follow a clear motif and alternate between two antipodal adsorption sites like the knight moves on a chessboard. The cation is always closely accompanied by the methyl and ethyl groups (the methyl group is generally somewhat closer; the propyl–cation separation lies merely in the direction perpendicular to the paper). Also the central carbon atom and the first carbon atom of the butyl group reside at short distances from the cation (< 4 Å), which is the optimal alkane–cation packing at the intersection.

The aluminum atoms in the Al-5 system are situated in pairs in diametrical positions in one of the 10-rings of the zigzag channels (see Figure 3). The Ca²⁺ ion counterbalances the negative charge and is therefore positioned between them. However, it is energetically more favorable to stay

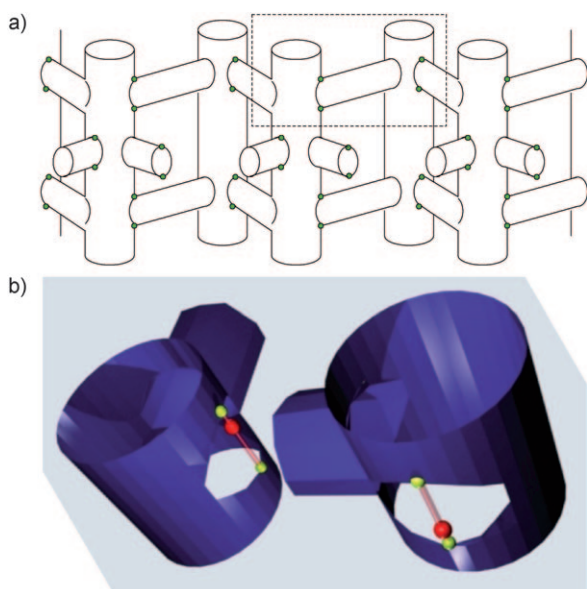


Figure 3. Illustration of “chiral cells”. a) Typical cylindrical representation of MFI. Large and small cylinders represent straight and zigzag channels, respectively. The green dots depict the Al positions. The dashed square is enlarged in panel b) showing the positions of aluminum atoms and cations at the channel intersections. The Ca^{2+} ion (red sphere) must choose between the two aluminum positions. The asymmetric positioning of the cation makes the exit channels distinctively different from each other. The differentiation in four spatial directions creates a local chiral environment that we call a “chiral cell”. In the neighboring intersection, the cation adopts the position that lies farthest away from the other cation. The induced chirality is therefore of the same type as in the other cell. The cells shown here preferentially adsorb the *S* enantiomer.

closer to one of them than to be in the exact middle. This results in two possible adsorption sites and the occurrence of what we call “chiral cells”. The asymmetric positioning of the cations, together with the presence of two different types of channels, makes the exit at the intersection physically different from each other and creates an effective chiral environment. This causes a mutual interaction; the positioning of the cation will favor one specific enantiomeric form. Vice versa, if either an *S* or *R* molecule is adsorbed in the cell, it will try to position the cation close to the aluminum atom, which suits it best. The cations, influenced by their electrostatic repulsion, try to maximize their separation. This induces nonlocal correlations between the cells (see Figure 3). Hypothetically, the adsorption of the first enantiomer would establish a chiral environment throughout the whole crystal, so that only molecules of the same type can enter. Under realistic thermodynamic conditions, the last statement should be viewed as an oversimplification; it does, however, correctly describe the main principle of why Al-5(Ca^{2+}) tends to favor that enantiomeric form that is already dominant in the reservoir.

The reason that some Al distributions did not show chiral discrimination can be explained by locations of aluminum atoms that are too far outside the channel intersections or a position of the cation that is not asymmetric.^[13]

Due to the slight commercial relevance of 4-ethyl-4-methyloctane and its expected low diffusivity in the MFI pore system, this is certainly not the ultimate system that one would like to put into practice. However, our simulation results provide a first proof-of-concept of a new kind of mechanism that is generally applicable to many other molecular systems. One relatively straightforward application is the purification of an enantioenriched feed, for instance, obtained from an asymmetric catalytic process.^[15] It is certainly not excluded that present-day zeolite materials inhibit the enantioselective effect that we describe. However, as our study shows, the efficiency of this type of selectivity would significantly profit from better control of substitution sites. Experimental determination of Al sites in MFI is a difficult task, though innovative techniques are underway.^[16–18] Our results are also valuable for this purpose, as isotherms like Figure 1 provide fingerprints of specific MFI frameworks, a feature that has not been achieved with adsorption studies using linear alkanes.^[19] A strict periodic ordering of aluminum atoms is presumably best, but the presence of some inhomogeneity in the system is not expected to annihilate the effect, as is supported by our analysis (see Supporting Information). In this respect, recent ^{27}Al NMR measurements are encouraging, as they suggest that specific Al distributions are created depending on the synthesis conditions, and that the number of occupied crystallographic T sites generally decrease with decreasing Si/Al ratio.^[17] Further experimental and theoretical research on the determination and control of substitution sites is highly appropriate, as mathematical modeling suggest that not only the purification but also the complete separation of scalemic mixtures becomes possible when the strength of enantioselective adsorption exceeds a certain limit.^[15] This would enable processes that, once initiated, no longer depend on an external source for the enantioenriched feed.

Received: October 29, 2009

Revised: January 8, 2010

Published online: March 18, 2010

Keywords: adsorption · chirality · computational chemistry · enantioselectivity · zeolites

- [1] G. Gübitz, M. G. Schmid, *Mol. Biotechnol.* **2006**, 32, 159–179.
- [2] J. F. M. Denayer, K. De Meyer, J. A. Martens, G. V. Baron, *Angew. Chem.* **2003**, 115, 2880–2883; *Angew. Chem. Int. Ed.* **2003**, 42, 2774–2777.
- [3] Y. Li, J. H. Yu, Z. P. Wang, J. N. Zhang, M. Guo, R. R. Xu, *Chem. Mater.* **2005**, 17, 4399–4405.
- [4] L. Q. Tang, L. Shi, C. Bonneau, J. L. Sun, H. J. Yue, A. Ojuva, B.-L. Lee, M. Kritikos, R. G. Bell, Z. Bacsik, J. Mink, X. D. Zou, *Nat. Mater.* **2008**, 7, 381–385.
- [5] J. L. Sun, C. Bonneau, A. Cantin, A. Corma, M. J. Diaz-Cabanas, M. Moliner, D. L. Zhang, M. R. Li, X. D. Zou, *Nature* **2009**, 458, 1154–U90.
- [6] P. A. Jacobs, J. A. Martens, *Stud. Surf. Sci. Catal.* **1987**, 33, 47.
- [7] H. Van Koningsveld, J. C. Jansen, H. Van Bekkum, *Zeolites* **1990**, 10, 235–242.
- [8] D. Dubbeldam, S. Calero, T. J. H. Vlugt, R. Krishna, T. L. M. Maesen, B. Smit, *J. Phys. Chem. B* **2004**, 108, 12301–12313.

- [9] S. Calero, D. Dubbeldam, R. Krishna, B. Smit, T. J. H. Vlugt, J. F. M. Denayer, J. A. Martens, T. L. M. Maesen, *J. Am. Chem. Soc.* **2004**, *126*, 11377–11386.
- [10] E. García-Pérez, D. Dubbeldam, T. L. M. Maesen, S. Calero, *J. Phys. Chem. B* **2006**, *110*, 23968–23976.
- [11] T. J. H. Vlugt, M. Schenk, *J. Phys. Chem. B* **2002**, *106*, 12757–12763.
- [12] M. G. Martin, J. I. Siepmann, *J. Phys. Chem. B* **1999**, *103*, 4508–4517.
- [13] T. P. Caremans, T. S. van Erp, D. Dubbeldam, J.-M. Castillo, J. A. Martens, S. Calero, submitted, **2009**.
- [14] T. S. van Erp, D. Dubbeldam, T. P. Caremans, S. Calero, J. A. Martens, submitted, **2009**.
- [15] T. S. van Erp, D. Dubbeldam, S. Calero, J. A. Martens, submitted, **2009**.
- [16] J. A. Van Bokhoven, T.-L. Lee, M. Drakopoulos, C. Lamberti, S. Thiss, J. Zegenhagen, *Nat. Mater.* **2008**, *7*, 551–555.
- [17] S. Sklenak, J. Dedecek, C. Li, B. Wichterlova, V. Gabova, M. Sierka, J. Sauer, *Phys. Chem. Chem. Phys.* **2009**, *11*, 1237–1247.
- [18] E. García-Pérez, D. Dubbeldam, B. Liu, B. Smit, S. Calero, *Angew. Chem.* **2007**, *119*, 280–282; *Angew. Chem. Int. Ed.* **2007**, *46*, 276–278.
- [19] B. Liu, E. Garcia-Perez, D. Dubbeldam, B. Smit, S. Calero, *J. Phys. Chem. C* **2007**, *111*, 10419–10426.